Computers and Chemical Engineering 96 (2017) 139–148

Contents lists available at ScienceDirect

Computers and Chemical Engineering

journal homepage: www.elsevier.com/locate/compchemeng

Optimal control of a laboratory binary distillation column via regionless explicit MPC

Ján Drgoňa, Martin Klaučo*, Filip Janeček, Michal Kvasnica

Institute of Information Engineering, Automation, and Mathematics, Slovak University of Technology in Bratislava, Radlinského 9, SK-812 37 Bratislava, Slovak Republic

ARTICLE INFO

Article history:
Received 30 May 2016
Received in revised form
22 September 2016
Accepted 12 October 2016
Available online 25 October 2016

Keywords:
Explicit predictive control
Optimization
Process control
Distillation

ABSTRACT

This paper shows how to construct and implement explicit MPC feedback laws for systems with a large number of states. Specifically, the construction of critical regions of the explicit MPC solution is replaced by a two-step procedure. First, all optimal active sets are enumerated off-line and corresponding KKT matrices are pre-factored. Then, in the on-line step, the optimal control inputs are identified by checking primal and dual feasibility conditions using the pre-factored data. The feasibility and performance of the proposed approach are experimentally demonstrated on the control of the laboratory binary distillation column, described by a dynamical model with 10 state variables. We show that the control algorithm requires only modest computational resources on-line. A comparison of the memory and computational demands of the proposed method with the on-line solution of the corresponding quadratic program via the state-of-the-art solver as well as the approximated solution via the first-order method is made.

1. Introduction

Distillation columns are often perceived as the flagships of process industries. They serve to separate the solutions of compounds into the individual components based on their different boiling point. The theoretical foundation of the operation of distillation columns can be found in many textbooks, e.g., in Gorak and Schoenmakers (2014), Perry and Green (2008). Since a significant amount of energy is required for the separation, energy-efficient control of distillation columns has received extensive attention by theoreticians and practitioners alike, see, e.g., (Skogestad, 1997, 2007) and references therein.

Predominantly, strategies based on model predictive control (MPC) are adopted for control of distillation columns since they allow to synthesize optimal control actions while simultaneously respecting constraints on manipulated variables and controlled outputs (Morari and Lee, 1999). It is worth noting that the well-known dynamic matrix control (DMC) approach was first developed in the context of control of distillation columns and oil refineries (Cutler and Ramaker, 1979). Other proposed strategies include, but are not limited to, robust MPC (Martin et al., 2013), adaptive MPC (Fileti and Pereira, 1997; Karacan et al., 1998), predictive master control strategies with PID slave controllers (Volk et al., 2005), nonlinear MPC (Nakaiwa et al., 1998; Kawathekar and Riggs, 2007), nonlinear MPC based on mixed-integer optimization (Meidanshahi, 2016), and intelligent control strategies (Fabro and Arruda, 2005), to name just a few.

A common disadvantage of existing MPC strategies is that the rely on solving a given optimization problem repeatedly at each sampling instant for updated values of the measurements of the plant. Although the MPC optimization is usually formulated as a convex quadratic program (QP) for which efficient solution techniques exist (Wang and Boyd, 2010; Richter et al., 2013; Herceg et al., 2015; Pu et al., 2016), the procedure still requires significant resources for its implementation in the control hardware. Specifically, two types of resources are required: computation and software. The first resource refers to a sufficient computational power being available to solve the QP at each sampling instant. Although distillation columns usually feature a slow dynamics, the computational factor can become a bottleneck when the control algorithm has to run on a hardware platform with limited computational resources. Examples of such platforms include programmable logic controllers (PLCs), which are frequently used in process industries (Huyck et al., 2014). The second type of resources – software – refers to the fact that to solve QPs on-line at each sampling instant, a suitable solver is required. This, in turn, requires a suitable operating system to be installed. Both of these components render the implementation more expensive when guarantees

* Corresponding author.
E-mail addresses: jan.drgona@stuba.sk (J. Drgoňa), martin.klauco@stuba.sk (M. Klaučo), filip.janecek@stuba.sk (F. Janeček), michal.kvasnica@stuba.sk (M. Kvasnica).

http://dx.doi.org/10.1016/j.compchemeng.2016.10.003
0098-1354/

on the accuracy of the solution are required. Moreover, solving QPs via active-set methods requires performing matrix inversions and divisions, which can render the implementation algorithm difficult to certify.

Both of these limitations can be addressed using the concept of explicit MPC (Bemporad et al., 2002; Pistikopoulos, 2012). Here, solving QPs on-line is avoided by pre-computing, off-line, the optimal solution using parametric programming. This gives rise to an analytical representation of the feedback law in the form of a piecewise affine (PWA) function defined over a set of polyhedral critical regions. Each such region defines the neighbourhood of the initial conditions where the same set of constraints is active. The main advantage of the explicit approach is that its on-line implementation boils down to a mere function evaluation. This is done by first performing the point location task, followed by the evaluation of the corresponding local affine function. This procedure is division-free (i.e., no matrix inversions are required), and therefore is trivial to implement in almost any programming language. Moreover, the code does not require any external libraries. However, the downside is that the construction of the critical regions is a time-consuming task, complexity of which scales badly with the dimensionality of the parametric space. Therefore it is ill suited to design MPC feedback strategies for distillation columns which typically feature 10 and more state variables.

Therefore in this paper we present the so-called *regionless* form of explicit MPC. It was first outlined in Borrelli et al. (2010) and later extended in our previous work Kvasnica et al. (2015).

The term *regionless* refers to two main features of the approach. First, unlike the geometric-based approaches of Bemporad et al. (2002), Pistikopoulos (2012), Baotic et al. (2008), here the critical regions are not required to construct the optimal feedback law. Instead, the feedback law is synthesized by a direct exploration of all feasible combinations of active constraints. As a consequence, the construction of the feedback law is no longer limited by the dimensionality of the parametric space as it was the case before. The second feature is that the regions are not even required for the subsequent on-line implementation of the explicit feedback law. Again, in geometric-based approaches the regions are vital in assigning the correct local affine feedback law to the state measurement. In the regionless approach, such an association is achieved by a direct evaluation of primal and dual feasibility conditions. A direct consequence of the on-line implementation not being based on critical regions is that the required memory storage is reduced considerably. It should be noted that if required (e.g. for analysis purposes), critical regions can still be recovered from the regionless format using the procedure presented in Kvasnica et al. (2015).

Technically speaking, the procedure consists of two steps. In the first step all locally optimal combinations of active constraints are obtained. In this paper this is done via the extensive enumeration approach of Gupta et al. (2011). Then, in the second step, the associated Karush–Kuhn–Tucker (KKT) system is partially pre-factorized for each optimal active set. This yields the analytic expression for the dual variables. Then the active sets along with the expressions for dual variables are stored in the control hardware. In the online phase, optimality of primal/dual candidates computed using pre-computed expressions are validated using primal/dual feasibility conditions. Compared to the approach of Borrelli et al. (2010), storing only the dual factors reduces the required memory footprint of the regionless solution. Results of the proposed regionless explicit MPC strategy are validated on an experiment which involves control of a laboratory distillation column with 8 trays (Armfield, 2010), described by the dynamical linear time-invariant state space model with 10 states.

This paper is a significant extension of our previous work Drgoňa et al. (2016). First, we provide a more detailed technical description of the regionless explicit MPC procedure. Furthermore, a detailed description of the hardware and software setups for the control of the distillation columns are presented. Finally, a comparison of the proposed regionless explicit MPC with fast on-line methods is presented. Here, first-order methods (Kouzoupis et al., 2015) implemented via the FiOrdOs toolbox (Ullmann, 2011) are considered, along with off-the-shelf optimization solvers represented by Gurobi (2012).

2. Plant description and modeling

This section provides the description of the distillation column and identification procedure necessary for obtaining sufficiently accurate linear time invariant model of the process.

2.1. Plant description

The scheme of the distillation column in shown in Fig. 1(a). The column operates by heating up the solution in a reboiler. From there, vapors of the more volatile substance rise through several trays of the column where they are enriched. Once they reach the head of the column, the enriched vapors are moved to the condenser where they are cooled down to a liquid state and collected in the distillate accumulator. The condensed enriched solution can either be fed back into the column or taken away as a product. The ratio between the portion of the liquid fed back and taken away is called the *reflux ratio* and represents the manipulated variable of the process. The column operates in a continuous manner with a preheated feed being constantly added to the system at a fixed flowrate.

The laboratory column considered in this paper separates the mixture of methanol and water, and is shown in Fig. 1(b). The column consists of 8 sieve plate trays with 50 mm diameter, divided into two glass sections, each containing four sieve plates. Trays are stacked one above the other and enclosed in a cylindrical shell to form a 2 m tall column. The whole column is insulated to minimize energy loss. The feed mixture is continuously injected on the fifth tray separating the column into the rectification and the stripping section, which are arranged vertically for counter-current vapor/liquid flow. The vapor, enriched by methanol molecules, stems from reboiler, and is directed through water cooled coil-in-shell condenser to distillate accumulator. Cooling water enters the condenser at a regulated rate through a variable area flow meter, controlled by a servo valve. The condensed product from the distillate accumulator is brought to reflux valve. The manipulated reflux ratio ranges between 0% and 100%. In this particular setup we are able to measure 10 signals, where $T_2, \ldots, T_9$ represent the temperatures at each tray of the column, while signal T_{10} represent the temperature in the reboiler and T_1 denoting the temperature at the top of the column. This quantity also represents the controlled variable. The purpose of the controller is to manipulate the reflux valve such that T_1 follows a user-defined reference.

The temperature on the head of the column can be correlated with the concentration of the more volatile substance (methanol in this case) via so-called *T-x-y* diagrams (Fig. 2). Therefore the desired product concentration can be directly translated to temperature references and vice versa. The objective here is to control the concentration of the methanol compound in the distillate. By the m_x is denoted the mole fraction of the methanol in the liquid phase, while by the mole fraction of the methanol in the vapor phase is expressed as m_y.

2.2. System identification

The dynamical behavior of the column in a neighborhood of the desired operating point can be sufficiently well approximated by a

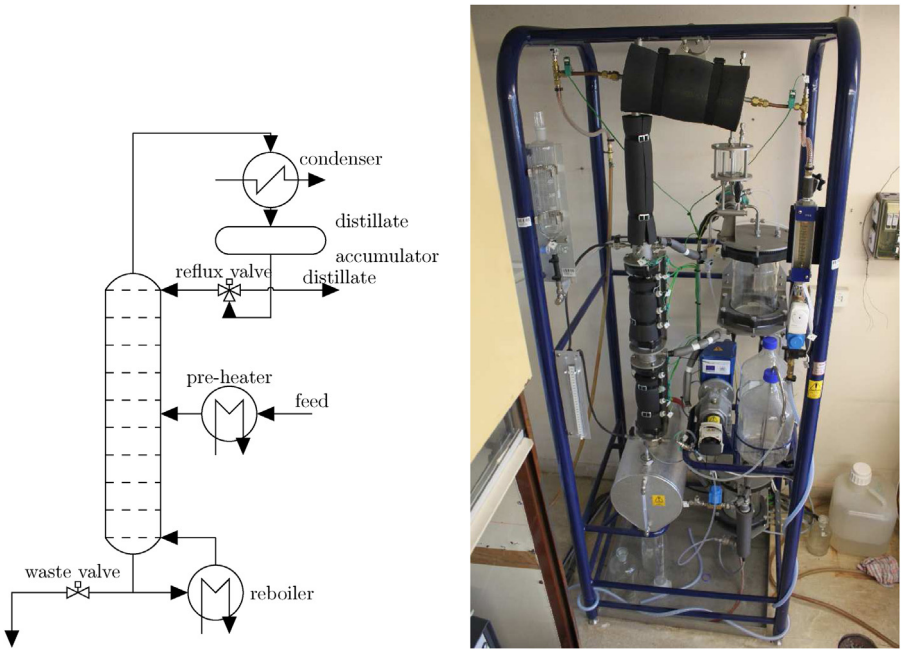

(a) Scheme of the distillation column unit. (b) The UOP3CC laboratory distillation column.

Fig. 1. The distillation column unit.

time-invariant linear system in the discrete-time domain

$$x_{k+1} = Ax_k + Bu_k, \tag{1a}$$

$$y_k = Cx_k. \tag{1b}$$

The system matrices A, B, and C were obtained by using system identification. Specifically, we have first performed a series of step changes of the manipulated reflux valve and measured the temperatures $T_1, \ldots, T_5$ in the enrichment part of the column at sampling frequency 1 Hz. Since the enrichment part of the distillation column is mostly susceptible to the changes in the reflux ratio, it is sufficient to consider only these five temperature measurements in the identification and subsequent control design.

The linear model (1) has been obtained for operating point given by steady state output values y^s. Furthermore, step changes in the whole range of reflux ratio [0, 100] % were considered in the identification procedure. The steady state values of the outputs are

$$y^s = \begin{bmatrix} 64.64 & 64.45 & 66.41 & 68.59 & 72.05 \end{bmatrix}^T {}^\circ\text{C}. \tag{2}$$

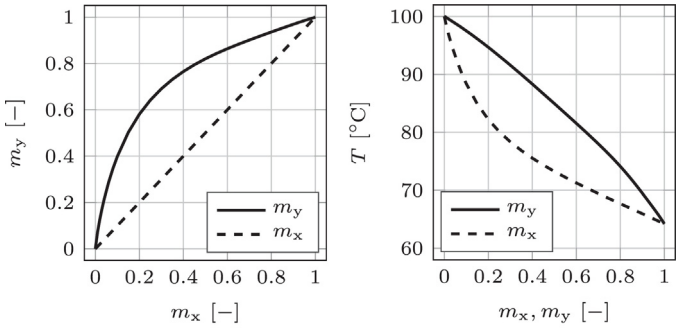

(a) $x - y$ (b) $T - x - y$

Fig. 2. Liquid–vapour equilibrium diagram of methanol–water solution at normal pressure p_0 = 101.325 kPa. The concentrations m_x, m_y are given in mole fractions.

Subsequently, the `n4sid` function of the System Identification toolbox for Matlab Ljung (1999) was used to find parameters of the model in (1). We have opted for a model with 10 states and 5 outputs, thus $A \in \mathbb{R}^{10\times10}$, $B \in \mathbb{R}^{10\times1}$ and $C \in \mathbb{R}^{5\times10}$. Matrices of the state-space model obtained via `n4sid` are reported in Appendix A as Eq. (A.1). The first order Butterworth filter with cut-off frequency equal to 0.005 rad s^{-1} was used in order to improve the accuracy of the identification procedure by filtering the high frequency noise present in the measured data. The accuracy of the identified model with respect to the measured response of the temperature at the head of the column T_1 is shown in Fig. 3. As can be seen, the 10-th order model captures the main dynamical characteristics with sufficient accuracy, with the overall goodness of the fit evaluated to ca. 85%.

It is important to note here, that the identified linear model is valid only near the operating point. Further compensation of

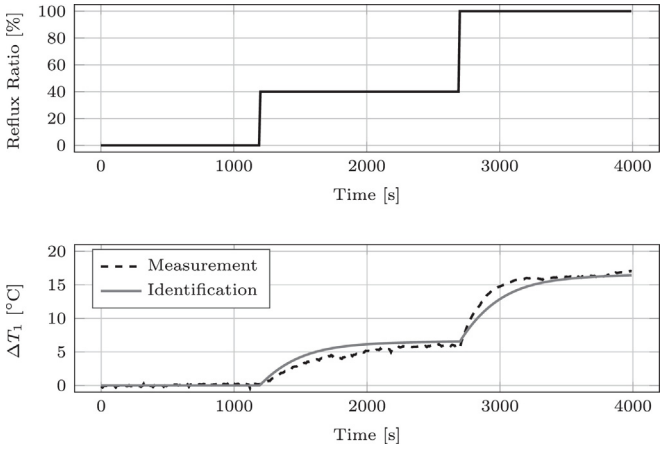

Fig. 3. Top figure; step changes of the reflux valve. Bottom figure: step responses of the measured temperature at the head of the column. The measurement is plotted as a deviation from a steady state.

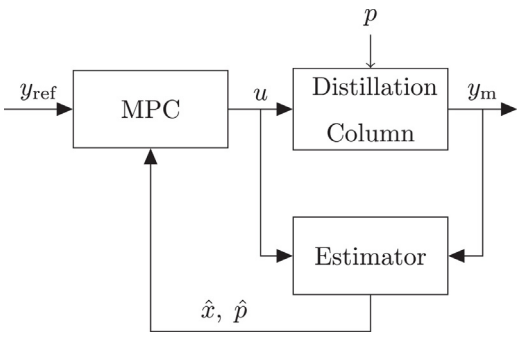

Fig. 4. Schematic representation of the closed-loop system. Here, p are unmeasured disturbances, y_m denotes the measured outputs, y_{ref} is the user-specified output reference, u is the control action, and $\hat{x}$, $\hat{p}$ denote the estimates of the plant's states and disturbances, respectively.

a plant-model mismatch will be obtained by the feedback action of the predictive controller with disturbance modeling and state estimation techniques (Muske and Badgwell, 2002).

3. Model predictive control setup

Fig. 4 shows the closed-loop system for control of the temperature at the head of the column. It consists of an MPC controller, the columns, and an estimator. The estimator is used to estimate the values of the states x and unmeasured disturbances. First, we report the design of the estimator in Section 3.1 before showing the MPC setup in Section 3.2.

3.1. State and disturbance estimation

To reject steady-state offset due to the plant-model mismatch, in this paper we use the offset-free reference tracking approach of Muske and Badgwell (2002). This approach extends the prediction model by an unmeasured disturbance p added to each output which is required to track the user defined reference. Therefore an extended model of the plant is considered:

$$x_{k+1} = Ax_k + Bu_k, \tag{3a}$$

$$y_k = Cx_k + Ep_k, \tag{3b}$$

$$p_{k+1} = p_k. \tag{3c}$$

Here, the disturbance vector p is assumed to have a constant dynamics (Pannocchia and Rawlings, 2003). The output disturbance matrix E was chosen as an identity matrix. Using this extended state model a state-space model of the estimator was designed as a stationary Kalman Filter in the form

$$\begin{bmatrix}\hat{x}\\ \hat{p}\end{bmatrix}_{k|k} = \begin{bmatrix}\hat{x}\\ \hat{p}\end{bmatrix}_{k|k-1} + L\left(y_m - \hat{y}_{k|k-1}\right), \tag{4a}$$

$$\begin{bmatrix}\hat{x}\\ \hat{p}\end{bmatrix}_{k+1|k} = \begin{bmatrix}A & 0\\ 0 & I\end{bmatrix}\begin{bmatrix}\hat{x}\\ \hat{p}\end{bmatrix}_{k|k} + \begin{bmatrix}B\\ 0\end{bmatrix}u_{k|k}, \tag{4b}$$

$$\hat{y}_{k|k} = \begin{bmatrix}C & E\end{bmatrix}\begin{bmatrix}\hat{x}\\ \hat{p}\end{bmatrix}_{k|k}. \tag{4c}$$

Here, the matrix L is the gain of the Kalman Filter and y_m denotes the measurements of the plant's outputs. The vectors $\hat{x}_k$, $\hat{y}_k$ and $\hat{p}_k$ then represent the estimated states, outputs, and disturbances of the augmented model, respectively.

The value of the estimator's gain matrix L was computed by a pole-placement method such that the matrix

$$\left(\begin{bmatrix}A & 0\\ 0 & I\end{bmatrix} - L\cdot\begin{bmatrix}C & E\end{bmatrix}\right) \tag{5}$$

has eigenvalues within the unit disc. The particular selection of the observer's gain used in the paper is reported in the Appendix in Eq. (A.1c).

3.2. MPC problem formulation

To control the column, the controller has to devise values of the reflux ratio which satisfy min/max constraints on its amplitude as well as on its increments, i.e.,

$$u_{min} \le \quad u(t) \le u_{max}, \tag{6}$$

$$\Delta u_{min} \le \quad \Delta u(t) \le \Delta u_{max}, \tag{7}$$

where $\Delta u(t) = u(t) - u(t-1)$. Moreover, the control inputs should steer the controlled output to a prescribed reference y_{ref}. Although the identified model in (1) (and its extended form in (3)) has 5 outputs, only the first output, i.e., T_1 (temperature at the head of the column) is controlled. The other four measured outputs were used solely to improve the performance of the state estimator.

These control objectives can be translated into the following MPC optimization problem:

$$\min_U \sum_{k=0}^{N_c-1} \|\Delta u_k\|^2_{Q_u} + \sum_{k=0}^{N} \|y_k - y_{ref}\|^2_{Q_y}, \tag{8a}$$

$$\text{s.t.} \quad x_{k+1} = Ax_k + Bu_k, \quad \forall k \in \mathbb{N}_0^{N-1}, \tag{8b}$$

$$y_k = \tilde{C}x_k + \tilde{E}p_0, \quad \forall k \in \mathbb{N}_0^{N}, \tag{8c}$$

$$u_k = u_{N_c-1}, \quad \forall k \in \mathbb{N}_{N_c}^{N-1}, \tag{8d}$$

$$\Delta u_k = u_k - u_{k-1}, \quad \forall k \in \mathbb{N}_0^{N_c-1}, \tag{8e}$$

$$u_{min} \le u_k \le u_{max}, \quad \forall k \in \mathbb{N}_0^{N_c-1}, \tag{8f}$$

$$\Delta u_{min} \le \Delta u_k \le \Delta u_{max}, \quad \forall k \in \mathbb{N}_0^{N_c-1}, \tag{8g}$$

where $\mathbb{N}_a^b = \{a, a+1, \ldots, b\}$ is a set of integers, x_k, u_k, y_k, denote, respectively, the k-th step predictions of the system's states, inputs, and outputs. Moreover, $\|z\|^2_M$ is the weighted squared 2-norm, i.e., $z^T M z$. The cost function (8a) employs the control horizon N_c and the prediction horizon N with $N_c \le N$. Therefore only the first N_c control moves, i.e., $u_0, \ldots, u_{N_c-1}$, are optimized. Afterwards, the control moves are blocked to the last predicted value via (8d). The first term of the cost function minimizes the fluctuations of the control input while the second term minimizes the tracking error. Note that for $k = 0$, (8e) becomes $\Delta u_0 = u_0 - u_{-1}$ where u_{-1} is the control input applied in the previous sampling instant. This quantity, together with the estimated initial state x_0, the output reference y_{ref}, and the estimated disturbance p_0 (which is assumed to be constant over the entire prediction horizon) constitute the initial conditions for (8).

Since only the first output is controlled, matrices $\tilde{C}$ and $\tilde{E}$ in (8c) were obtained by only retaining the first row of C and E used in (3). As a consequence, p_0 is a scalar unmeasured disturbance.

The closed-loop implementation of the MPC strategy represented by (8) then follows standard principles of receding horizon control:

1 Measure the plant's output $y_m(t)$ and estimate the current value of the state $\hat{x}(t)$ and the unmeasured disturbance $\hat{p}(t)$ via (4).
2 Solve (8) for initial conditions $x_0 = \hat{x}(t)$, $p_0 = \hat{p}(t)$, $u_{-1} = u^\star(t-1)$, and for a given value of the output reference y_{ref}. Obtain the open-loop optimal control sequence $U^\star = \{u_0^\star, \ldots, u_{N_c-1}^\star\}$.
3 Set $u^\star(t) = u_0^\star$ and apply it to the plant.
4 Continue with Step 1 at the next sampling instant.

Since the objective function in (8a) is quadratic and all constraints are linear, problem (8) can be solved as a quadratic program (QP). However, solving QPs on-line at every sampling instant

requires sufficient computational (e.g., time and power) and software (e.g., solvers and libraries) resources. Therefore in the next section, we show how to obtain the optimal control inputs using fewer computational and software resources, thus allowing for a cheaper implementation of MPC.

4. Explicit regionless model predictive control

In this section, we show how to derive the analytical solution to the MPC problem in (8) in the form of a function which maps the initial conditions onto optimal control inputs. Contrary to traditional explicit MPC techniques based on parametric programming, the approach presented here requires neither the computation, nor the storage of so-called *critical regions*. By avoiding construction and storage of the regions, we are able to construct the analytical solution faster even for large dimensions of the parametric space. Moreover, the regionless solution of this section consumes less space compared to region-based approaches.

Let $U = [u_0^T, \ldots, u_{N_c-1}^T]^T$ be the vector of open-loop input predictions and $\theta = [x_0^T, u_{-1}^T, y_{\text{ref}}^T, p_0^T]^T$ be the vector of initial conditions for (8). After straightforward algebraic manipulations, the MPC problem (8) can be translated into

$$\min_U 1/2 \quad U^T H U + \theta^T F U \tag{9a}$$

$$\text{s.t.} \quad GU \leq w + S\theta, \tag{9b}$$

which is a parametric quadratic program (pQP). Under the assumption that $Q_u = Q_u^T \succ 0$ and $Q_y = Q_y^T \succ 0$ in (8a), the Hessian H in (9a) will be symmetric and positive definite, thus invertible.

Our objective is to devise a scheme which computes the optimal open-loop control sequence $U^\star$ without having to solve (9) numerically, on-line, for a particular value of the vector of initial conditions θ. Specifically, we show that the optimal map $\theta \to U^\star$ can be computed off-line.

Remark 4.1. All procedures of this section can be applied to generic pQP problems of the form (9) and are thus not limited to the specific formulation in (8). □

Our approach is based on two steps. In the first one, all combinations of constraints that can possibly be active and locally optimal for some neighborhood of parameters in (9) is enumerated off-line. Unlike "traditional" region-based explicit MPC approaches, this neighborhood needs not be explicitly characterized in the form of a polyhedral critical region. Then, in the second step, for each locally optimal active set we construct the maps $g_i : \theta \to U^\star$ where the subindex i denotes the i-th locally optimal active set.

Both steps rely on Karush–Kuhn–Tucker conditions of the pQP (9):

$$HU^\star + F^T\theta + G_{\mathcal{A}}^T\lambda^\star = 0, \tag{10a}$$

$$G_{\mathcal{A}}U^\star = w_{\mathcal{A}} + S_{\mathcal{A}}\theta, \tag{10b}$$

$$G_{\mathcal{N}}U^\star < w_{\mathcal{N}} + S_{\mathcal{N}}\theta, \tag{10c}$$

$$\lambda^\star \geq 0, \tag{10d}$$

$$\lambda^{\star T}(G_{\mathcal{A}}U^\star - w_{\mathcal{A}} - S_{\mathcal{A}}\theta) = 0, \tag{10e}$$

where λ are the dual variables, and $G_{\mathcal{A}}$ represents the matrix created by retaining from G only the rows indexed by the set of active constraints $\mathcal{A} \subseteq \{1, \ldots, n_c\}$ where n_c is the number of rows of G. Similar notations is used for $w_{\mathcal{A}}$ and $S_{\mathcal{A}}$. Moreover, $\mathcal{N}$ denotes the set of inactive constraints, i.e., $\mathcal{N} = \{1, \ldots, n_c\} \backslash \mathcal{A}$.

To enumerate all possible active sets $\{\mathcal{A}_1, \ldots, \mathcal{A}_R\}$ which can be locally optimal for (9) we suggest to use the *extensive enumeration* procedure proposed in Gupta et al. (2011). There, all optimal active sets are generated by exploring all combinations of active constraints in a branch-and-bound fashion. Infeasibility of a particular combination is used in the bounding phase to cut away branches of the exploration tree and thus to reduce the exploration complexity, cf. Fig. 5. To determine feasibility of a candidate active set, a linear program (LP) based on the KKT conditions (10) needs to be solved. In the worst case, there are

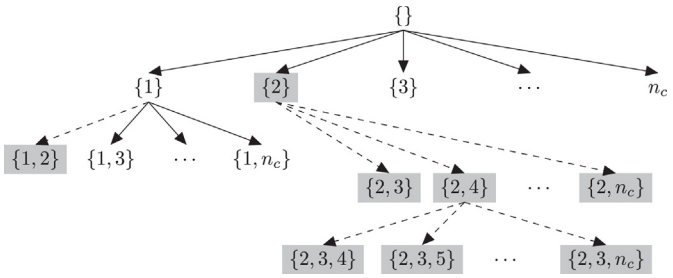

Fig. 5. Illustration of the extensive enumeration branch-and-bound approach of Gupta et al. (2011). If a particular combination of active constraints is infeasible, all nodes containing such a combinations can be eliminated from the exploration.

$$R_{\max} = \sum_{k=0}^{|U|} \frac{n_c!}{k!(n_c-k)!} \tag{11}$$

candidate active sets to check for feasibility. Here, $|U|$ is the number of optimization variables (for the specific formulation in (8), $|U| = N_c n_u$ where N_c is the control horizon in (9) and n_u is the number of control inputs of the system) and n_c is the number of constraints in (9b). It should be noted that, in our experience, the number of locally optimal active sets, i.e., R, satisfies $R \ll R_{\max}$. However, the exact value of R is entirely problem-specific.

Subsequently, in the second stage we take the list of active sets generated previously and for each of its element we compute the locally optimal map $\theta \to U^\star$. Specifically, for each locally optimal active set $\mathcal{A}$ we have

$$U^\star = -H^{-1}(F^T\theta + G_{\mathcal{A}}^T\lambda^\star) \tag{12}$$

directly from (10a) by the assumed invertibility of the Hessian. Substituting (12) into (10b) we obtain[1]

$$\lambda^\star = -(G_{\mathcal{A}}H^{-1}G_{\mathcal{A}}^T)^{-1}\left(w_{\mathcal{A}} + (S_{\mathcal{A}} + G_{\mathcal{A}}H^{-1}F^T)\theta\right), \tag{13}$$

which can be written as

$$\lambda^\star = Q(\mathcal{A})\theta + q(\mathcal{A}) \tag{14}$$

with

$$Q(\mathcal{A}) = -(G_{\mathcal{A}}H^{-1}G_{\mathcal{A}}^T)^{-1}(S_{\mathcal{A}} + G_{\mathcal{A}}H^{-1}F^T), \tag{15a}$$

$$q(\mathcal{A}) = -(G_{\mathcal{A}}H^{-1}G_{\mathcal{A}}^T)^{-1}w_{\mathcal{A}}. \tag{15b}$$

$Q(\mathcal{A}_i)$ and $q(\mathcal{A}_i)$ can be pre-computed off-line for each locally optimal active set $\{\mathcal{A}_1, \ldots, \mathcal{A}_R\}$. In the on-line phase these expressions are then used to to obtain $U^\star$ associated to a given initial condition θ. This is done by first determining which active set is optimal for a given θ. This can be achieved by traversing through the list of locally optimal active sets is a sequential order, as described in Algorithm 1.

[1] At this point we assume that the pQP (9) is either not degenerate, in which case $G_{\mathcal{A}}$ is of full row rank, or that at most $|\mathcal{A}|$ linearly independent rows are obtained from $G_{\mathcal{A}}$, see (Spjøtvold et al., 2005).

Algorithm 1. Evaluation of the regionless explicit MPC solution

```
procedure REGIONLESS(θ)                          ▷ given initial condition θ
    for i ∈ {1, ..., R} do
        Compute λ = Q(A_i)θ + q(A_i)
        if λ ≥ 0 then                            ▷ dual feasibility check
            Compute U = −H^{-1}(F^T θ + G_{A_i}^T λ)
            if GU ≤ w + Sθ then                  ▷ primal feasibility check
                U* ← U
                return U*                        ▷ obtain globally optimal U*
            end if
        end if
    end for
end procedure
```

Remark 4.2. Note that the Hessian H is constant, therefore its inverse H^{-1} used in (12) can be pre-computed off-line. □

The sequential algorithm outlined above is very simple and can be implemented in 10 lines of code in C. Moreover, the implementation is division-free as it does not require any matrix inversions, cf. Remark 4.2. Therefore no special libraries are required for its implementation. The algorithm utilizes pre-computed matrices $Q(\mathcal{A}_i)$, $q(\mathcal{A}_i)$, the list of active sets $\mathcal{A}_i, i \in \{1, \ldots, R\}$, as well as the pQP data H, F, G, w, and S as its data.

Remark 4.3. A similar procedure was also proposed in (Borrelli et al., 2010). However, the algorithm presented there requires more memory space since it also relies on characterizing $U^\star$ in (12) explicitly as $U^\star = V(\mathcal{A})\theta + v(\mathcal{A})$, followed by storing the matrices $V(\mathcal{A})$, $v(\mathcal{A})$ for each locally optimal active set. In our approach this additional storage is avoided by evaluating $U^\star$ directly from (12) once $\lambda^\star$ is computed via (14). □

5. Experimental results

In this section we present the experimental results of the regionless explicit MPC for the distillation column. First we present the computational complexity and the memory demands of the proposed solution, comparing it with the on-line solutions of the corresponding QP solved via state of the art optimization algorithms and approximated first-order methods. The description of the hardware and software setups follows, and finally, experimentally collected data are introduced. The objectives of the experiment are:

- Tutorial demonstration of a closed loop implementation of a regionless explicit MPC controller on a laboratory distillation process.
- Adjust the parameters of the predictive controller for optimal performance of the controlled process.
- Observe the reference tracking and disturbances rejection capabilities of the designed controller.
- Comparison of the memory and the computational demands of the regionless explicit MPC with the on-line MPC solutions.

5.1. Controller synthesis and complexity

We have applied the proposed regionless explicit MPC formulation to devise a controller for the column described by a state-space model with 10 states. The vector of initial conditions for (8) is $\theta = [\hat{x}(t)^T, u(t-1), y_{\text{ref}}, \hat{p}(t)]^T$, where $\hat{x}(t) \in \mathbb{R}^{10\times 1}$ is the estimate of the current plant's state, $u(t-1) \in \mathbb{R}^{1\times 1}$ is the control input applied at the previous sampling instant, $y_{\text{ref}} \in \mathbb{R}^{1\times 1}$ is the current value of the output reference, and $\hat{p}(t) \in \mathbb{R}^{1\times 1}$ is the estimate of the disturbance. Therefore $\theta \in \mathbb{R}^{13\times 1}$, and the dimension of the parametric space of the pQP (9) is thus 13.

To obtain the regionless representations of the explicit MPC feedback, we have used three differently weighted setups with $N = 40$, $N_c = 5$, $Q_u = 1$, $Q_y = \{200, 300, 400\}$, $u_{\min} = 0$, $u_{\max} = 100$, $\Delta u_{\min} = -10$, and $\Delta u_{\max} = 10$ in (8). With these settings, the pQP in (9) has 26 constraints. The subsequent extensive enumeration of locally optimal active sets showed that there were $R = 1095$ such combinations (we remark that $R_{\max} = 83,682$, cf. (11)). The enumeration, which included feasibility checks (10) and construction of $\mathcal{Q}(\mathcal{A})$, $q(\mathcal{A})$ per (15), took 6 s on a 1.70 GHz machine using the Multi-Parametric Toolbox (Herceg et al., 2013).

The pre-computed regionless explicit solutions consist of the list of optimal active sets $\mathcal{A}_1, \ldots, \mathcal{A}_R$, the associated expressions for the dual variables $Q(\mathcal{A}_i)$, $q(\mathcal{A}_i)$ per (15), and the matrices H, F, G, w, E of the pQP (9). The 1095 active sets require 3918 integers for their storage. Moreover, 54,852 floating point numbers are required to store $Q(\mathcal{A}_i)$, $q(\mathcal{A}_i)$, along with 584 floating point numbers for the pQP matrices. Assuming that 2 bytes are needed to store an integer and 4 bytes for a single-precision floating point number, the total memory footprint of the proposed single regionless explicit MPC solution is 224 kilobytes.

For the sake of completeness, we have also applied the geometric region-based method to synthesize the explicit MPC solution. Specifically, we have used the parametric solver contained in the MPT toolbox (Herceg et al., 2013), but similar algorithms can also be found in the POP toolbox (Pistikopoulos et al., 2015). The region-based explicit MPC solution is defined over 1095 critical regions which require a massive 10004490 floating-point numbers for their storage. This translates to 40 megabytes of data. Compared to 224 kilobytes of data for the regionless solution, this illustrates that a two order of magnitude reduction with respect to memory storage can be achieved by using the procedures of this paper. Moreover, it took 360 s on a 1.70 GHz machine to synthesize the region-based solution, an increase by a factor of 60 compared to the regionless solution. All data are summarized in Table 1.

For the comparison of the proposed regionless method with approaches based on on-line implementation, we have formulated the MPC problem in YALMIP (Löfberg, 2004). The resulting QP was subsequently solved in each sampling instant via the

Table 1
The off-line construction time and storage demands of the explicit MPC approaches.

Method	Construction time	Memory demands
Regionless	6 s	224 kB
Region-based (Bemporad et al., 2002; Baotic et al., 2008)	360 s	40 MB

Table 2
The on-line computational time and solution accuracy comparison of the investigated MPC approaches.

On-line method	Worst case CPU time	Sub-optimality
Regionless MPC via Algorithm 1	1.95 ms	0.00[%]
Region-based MPC	2.24 ms	0.00[%]
FiOrdOs (Ullmann, 2011)	13.00 ms	0.04[%]
Gurobi (Gurobi, 2012)	38.74 ms	0.00[%]

state-of-the-art optimization solver Gurobi (Gurobi, 2012). Moreover, fast first-order methods implemented via the FiOrdOs (Ullmann, 2011) package were compared as well. In the latter case, the maximum number of iterations was set to 1000, and the gradient-map stopping criterion was equal to $1 \cdot 10^{-8}$. The computational time demands and the solution accuracy comparison are summarized in Table 2. As can be seen, the regionless explicit MPC outperforms all alternatives. Specifically, its online runtime is by 15% smaller compared to the region-based explicit solution where the point-location task was implemented as a sequential search.[2] More importantly, the proposed regionless solution performs one order of magnitude better than the state-of-the-art solver as well as the fast first-order algorithm. The evaluation of the regionless explicit MPC solution was performed by translating Matlab implementation of Algorithm 1 into the C language via the `codegen` framework of Matlab. All algorithms ran on an Intel CORE i7 2.3 GHz machine under a 64-bit GNU/Linux 3.13.0 operating system.

5.2. HW and SW setup

The distillation column unit described in Section 2 is connected to a bench-mounted UOP3CC control console (Armfield, 2010) via a multi-conductor cable. The unit serves to measure temperatures at the individual trays of the column, which are subsequently used for the state estimation. The temperatures are measured by thermocouple sensors and subsequently converted by the control console to unified signals 0–5 V, representing the temperature span 0–150°C.

The reboiler, which heats the solution at the bottom of the column, consist of a flameproof immersion type heating element with maximum power of 2.5 kW, and a storage tank with the capacity of 20 l. The heating element provides heating power to the mixture, heating it up to the desired boiling temperature, which is approximately 90°C. The UOP3CC console directly controls the input power entering the reboiler via an input signal 0–5 V, which represents heating power 0–2.5 kW. The second heat exchanger in the process unit is the feed pre-heater providing heating power to the mixture entering the column on the 5-th tray. This electrical heat exchanger with a maximum power of 2 kW was installed as an extra device, as it was not originally part of the process unit. The control of pre-heaters input power requires, therefore, an additional power circuit to be present in the instrumentation. This power circuit consist of wiring and a solid-state relay which generates a pulse width modulated (PWM) binary electrical signal.

[2] Due to the size of the parametric solution (13 parameters and 1095 regions), it was not possible to apply a more sophisticated point location algorithm, such as a binary search tree (Tøndel et al., 2003).

The process unit also contains a feed pump whose speed is precisely controlled in the range 0–300 RPM via a variable frequency drive (VFD) contained in the control console. Finally, the unit contains two solenoid valves which control the liquid flows in individual parts of the column. The waste valve is operated by a voltage signal where 0 V represents the fully closed and 24 V the fully open positions. In our experiment, the valve was constantly open to maintain a constant level of the mixture in the reboiler.

The reflux solenoid three-way on-on valve (diverter) operates in a binary manner, i.e., either the whole distillate is removed from the column as a product, or it is fully returned back to the top of the column as the reflux. The control signal for the reflux valve is generated by the control console's relay card via a PWM signal. The DC signals corresponding to this setup are then as follows: 0 V for reflux flow and 24 V for the product flow. Therefore the continuous control signal representing the optimal reflux ratio generated by the MPC controller is first approximated by a PWM signal with frequency 1 Hz. The MPC algorithm ran on the sampling. This inherent physical limitation of the process then slightly reduces the control performance.

Finally, the signals from the control console and from the power circuits are fed via a multi-conductor cable to two I/O PC cards (MF 624) connected to the host PC, which executes state estimation and the control algorithm. All signal processing and necessary computations were done in Matlab and Simulink. The overall electrical instrumentation and wiring scheme is shown in Fig. 6.

Measurements and control evaluation was realized based on a steady state value of the measured outputs (2), equal to an operational point for identification. The steady state was maintained by setting the waste valve opening, the flow rate, the flow rate and the reboiler power to a constant value. Specifically the waste valve was fully open, the reboiler power was set to 0.73 kW and the flow rate of the feed was 1 mL s^{-1}. The temperature of the feed was maintained the same value as was the temperature of the mixture on the fifth tray.

5.3. Experimental results

This section presents experimentally collected data under the proposed regionless explicit MPC strategy. We remind that the objective of the controller is to optimally operate the reflux valve such that the temperature at the head of the column follows a prescribed reference. To show the performance of the controller, a series of step changes of the reference was performed with the steady state $y^s = 65\,^\circ$C taken as a starting point. Three consecutive steps with increase of the reference temperature by 5 °C were performed, each in an approximate duration of 10 min, followed by a step with the decrease of reference temperature by 5 °C. The step changes were intentionally chosen to cover the whole operational range of the temperatures at the top of the column.

The experimentally collected data for three control setups are reported in Figs. 7–9. Specifically, Figs. 7(a), 8(a) and 9(a) show the closed-loop response of the temperature on the top of the column with respect to step changes of the reference signal. The corresponding profile of the optimal control actions devised by the regionless explicit MPC controller are shown in Figs. 7(b), 8(b) and 9(b). Naturally, constraints on the amplitude of the control action as well as on its slew rate are respected since they were explicitly accounted for in (8). The small chattering of the outputs and inputs is caused by measurement noise as well as by the binary nature of the reflux valve. The main reason for a slight offset in the last stage of the experiments stems from the nonlinearity of the controlled process. Worth noting is that the settling time of regionless MPC controller with $Q_y = 400$ from Fig. 9 was 240 s, which is approximately 3 times faster than the open-loop response, cf. Fig. 3, which is 750 s. The overall comparison of the performance

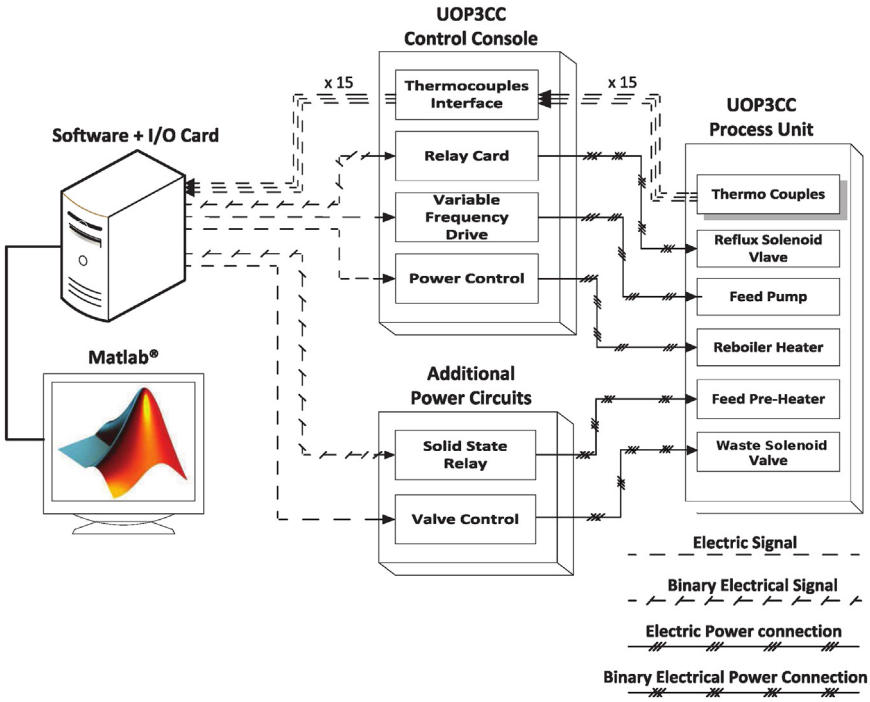

Fig. 6. Electrical instrumentation and wiring scheme for the UOP3CC laboratory distillation column.

of individual regionless MPC controllers with different weighting parameter Q_y via various criteria is shown in Table 3. We choose two reference tracking performance criteria, where ISE denotes the integral square error per sampling instant and IAE stands for integral absolute error per sampling instant. As expected, with increasing weighting parameter Q_y we were able to improve the reference tracking performance criteria as shown in Table 3. For evaluation of product quantity, we use the integral of the control action divided by a number of sampling instants, resulting in average control action per sampling instant (ACA), which directly accounts for the amount of the distillate being taken out as a product. In our control setup, the higher control actions will provide higher product quantity. It is important to note that for setup with $Q_y = 300$, the significantly greater value of the ACA quality criterion was caused by slightly higher initial steady state temperature measurement. This offset can be seen on the Fig. 8(a) and the difference

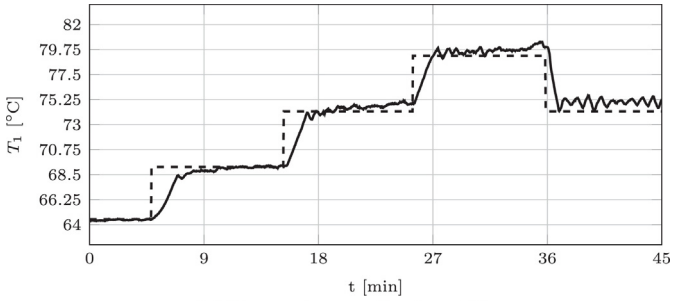

(a) Temperature profile $Q_y = 200$

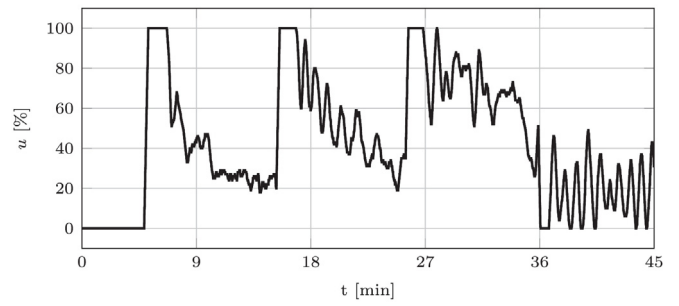

(b) Control action profile $Q_y = 200$

Fig. 7. Control setup for explicit MPC controller with $Q_y = 200$. Top figure: response of the temperature on the top of the column (solid) with respect to the desired reference (dashed). Bottom figure: profile of the control actions.

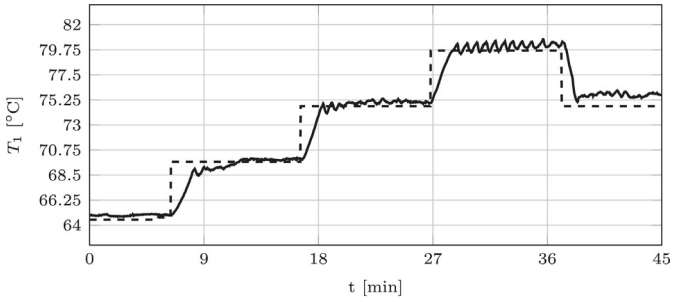

(a) Temperature profile $Q_y = 300$

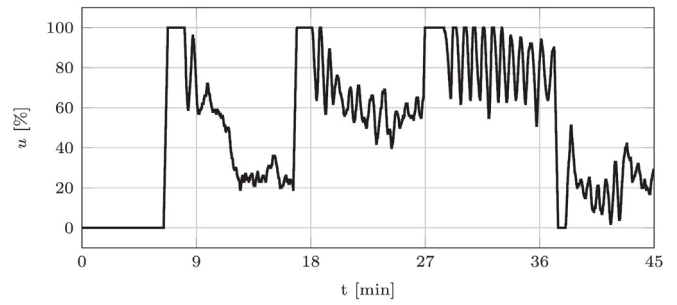

(b) Control action profile $Q_y = 300$

Fig. 8. Control setup for explicit MPC controller with $Q_y = 300$. Top figure: response of the temperature on the top of the column (solid) with respect to the desired reference (dashed). Bottom figure: profile of the control actions.

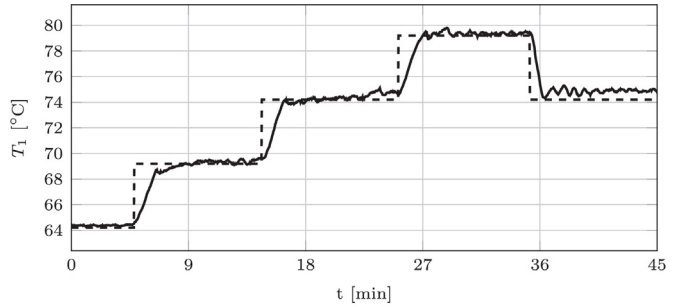

(a) Temperature profile $Q_y = 400$

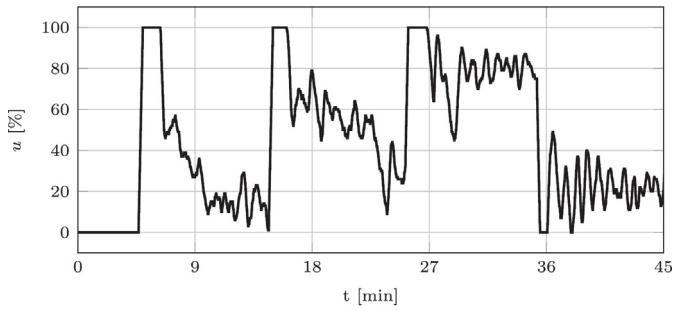

(b) Control action profile $Q_y = 400$

Fig. 9. Control setup for explicit MPC controller with $Q_y = 400$. Top figure: response of the temperature on the top of the column (solid) with respect to the desired reference (dashed). Bottom figure: profile of the control actions.

Table 3
The performance criteria comparison of the MPC controllers with different weighting parameter Q_y.

MPC setup	ISE [°C^2]	IAE [°C]	ACA [%]
$Q_y = 200$	1.8186	0.7896	48.5967
$Q_y = 300$	1.7899	0.7711	56.3489
$Q_y = 400$	1.3643	0.6183	49.6765

in the initial steady state value of the temperature originates in the higher temperature of the skeleton of the laboratory device.

6. Conclusions

In this paper, we have shown how to control a distillation column using an MPC algorithm. To allow for a fast and simple implementation of the control strategy, we have used the regionless explicit approach. Specifically, the feedback law was pre-computed off-line. To avoid the curse of dimensionality typical for the storage requirements of explicit MPC strategies, we have used the direct enumeration of all optimal combinations of active constraints. Moreover, the complexity of the analytical feedback law was kept low by only considering a partial pre-factorization of the KKT system for dual variables. Then the optimal control actions can be obtained by a sequential search procedure, which only needs to check primal and dual feasibility via a series of matrix multiplications and additions. Therefore the whole implementation is division free, fast, and simple to implement.

The main advantage of the regionless approach over region-based approaches is twofold. First, the construction of the analytical form of the MPC feedback law does not directly depend on the dimensionality of the parametric space. Therefore such solutions can be obtained even for systems with a high number of system's states. Secondly, as documented in Section 5.1, the regionless solution requires a significantly smaller memory footprint compared to its region-based alternative. Specifically, the required memory storage is decreased by two orders of magnitude.

The computational complexity of the proposed approach was compared with the standard and approximated on-line solutions of the corresponding QP via the state of the art optimization solvers. The results showed that regionless explicit approach can indeed provide significant computational improvements, outperforming the standard on-line QP solution roughly by the factor of 19, with no additional cost to be paid in the sub-optimality of the computed solution. By means of an experiment we have demonstrated that the proposed MPC controller achieves a suitable control performance. The influence of the model-plant mismatch was mitigated by using the disturbance modeling approach.

Acknowledgments

The Authors gratefully acknowledge the contribution of the Slovak Research and Development Agency under the project APVV-15-0007, and the financial support of the of the Scientific Grant Agency of the Slovak Republic under the grants 1/0403/15.

Appendix A. Model parameters

Particular values of the matrices A, B, C of the model in (1) obtained by system identification, along with the observer's gain matrix L in (4) are reported in (A.1a)– (A.1c).

$$A = \begin{bmatrix} 0.9970 & -0.0008 & -0.0001 & -0.0009 & 0.0020 & -0.0006 & 0.0005 & -0.0019 & -0.0010 & -0.0025 \\ -0.0006 & 0.9999 & 0.0002 & 0.0006 & -0.0002 & 0.0003 & 0.0021 & -0.0018 & -0.0018 & -0.0018 \\ 0.0013 & 0.0003 & 0.9977 & 0.0018 & -0.0002 & -0.0007 & -0.0023 & 0.0020 & 0.0038 & 0.0041 \\ 0.0032 & -0.0004 & -0.0018 & 0.9940 & -0.0036 & 0.0318 & -0.0008 & 0.0042 & 0.0019 & 0.0121 \\ 0.0007 & 0.0003 & 0.0002 & -0.0163 & 0.8041 & 0.5906 & -0.0002 & 0.0625 & 0.0191 & 0.0723 \\ 0.0007 & -0.0006 & 0.0004 & -0.0261 & -0.5842 & 0.8089 & -0.0008 & -0.0292 & -0.0229 & -0.0185 \\ 0.0011 & -0.0016 & 0.0023 & -0.0023 & -0.0025 & -0.0001 & 0.9911 & 0.0141 & -0.0086 & 0.0149 \\ 0.0019 & 0.0002 & 0.0016 & -0.0063 & -0.0106 & -0.0130 & -0.0157 & 0.2994 & -0.9139 & 0.2570 \\ -0.0003 & 0.0007 & -0.0018 & 0.0062 & -0.0254 & 0.0013 & -0.0079 & 0.8916 & 0.1581 & -0.3229 \\ -0.0001 & -0.0003 & 0.0034 & -0.0046 & 0.0300 & 0.0145 & 0.0080 & 0.0741 & 0.0116 & -0.4568 \end{bmatrix}, \quad \text{(A.1a)}$$

$$C = \begin{bmatrix} 240.0779 & 112.7997 & 11.2734 & 1.7447 & -3.6158 & -1.3766 & -0.6259 & 3.6039 & 3.0660 & 2.1594 \\ 247.6920 & 96.2199 & -7.6288 & -14.1476 & -2.9245 & -1.3406 & 3.8997 & 3.7248 & 2.8317 & 2.1730 \\ 289.5420 & -25.0577 & -20.8149 & 0.8503 & -6.2657 & -1.4946 & -4.4291 & 3.4022 & 3.2462 & 1.9510 \\ 281.8938 & -113.0640 & 1.3608 & 6.2130 & -6.2830 & -1.5922 & 6.7079 & 3.4677 & 2.9192 & 1.8208 \\ 232.0810 & -138.2255 & 23.7108 & -9.6844 & -5.2642 & -1.4766 & -4.2775 & 3.3838 & 3.0100 & 1.4844 \end{bmatrix}, \quad \text{(A.1b)}$$

$$B = 10^{-3} \cdot \begin{bmatrix} 0.0025 \\ 0.0009 \\ -0.0018 \\ -0.0058 \\ -0.0380 \\ -0.0047 \\ -0.0023 \\ 0.0337 \\ 0.1293 \\ 0.2131 \end{bmatrix},$$

$$L = \begin{bmatrix} 0.0009 & 0.0011 & -0.0002 & 0.0022 & -0.0003 \\ 0.0038 & 0.0008 & -0.0002 & -0.0023 & -0.0017 \\ 0.0174 & -0.0061 & -0.0204 & 0.0011 & 0.0127 \\ 0.0293 & -0.0389 & 0.0057 & 0.0207 & -0.0212 \\ -0.0101 & 0.0264 & -0.0430 & 0.0460 & -0.0204 \\ -0.0232 & 0.0448 & -0.0553 & 0.0566 & -0.0251 \\ -0.0190 & 0.0368 & -0.0482 & 0.0551 & -0.0263 \\ -0.0012 & 0.0034 & -0.0008 & -0.0054 & 0.0057 \\ 0.0036 & -0.0056 & 0.0064 & -0.0088 & 0.0051 \\ -0.0002 & 0.0008 & -0.0012 & 0.0009 & -0.0002 \\ 0.0276 & -0.0319 & 0.0091 & 0.0001 & -0.0029 \\ -0.0228 & 0.0434 & -0.0329 & 0.0094 & 0.0089 \\ -0.0160 & 0.0041 & 0.0313 & -0.0245 & 0.0047 \\ -0.0092 & 0.0137 & -0.0265 & 0.0421 & -0.0223 \\ 0.0100 & -0.0178 & 0.0228 & -0.0402 & 0.0291 \end{bmatrix}. \quad \text{(A.1c)}$$

References

2010. Armfield, Continuous Distillation Column, Armfield UOP3CC Instruction Manual. www.armfield.co.uk.

Baotic, M., Borrelli, F., Bemporad, A., Morari, M., 2008. Efficient on-line computation of constrained optimal control. SIAM J. Control Optim. 47 (5), 2470–2489.

Bemporad, A., Morari, M., Dua, V., Pistikopoulos, E.N., 2002. The explicit linear quadratic regulator for constrained systems. Automatica 38 (1), 3–20.

Borrelli, F., Baotić, M., Pekar, J., Stewart, G., 2010. On the computation of linear model predictive control laws. Automatica 46 (6), 1035–1041.

Cutler, C.R., Ramaker, B.L., 1979. Dynamic matrix control – a computer control algorithm. In: AICHE National Meeting, Houston, TX.

Drgoňa, J., Janeček, F., Klaučo, M., Kvasnica, M., 2016. Regionless explicit MPC of a distillation column. In: IEEE European Control Conference.

Fabro, J.A., Arruda Jr., L.F.N., 2005. Startup of a distillation column using intelligent control techniques. Comput. Chem. Eng. 30, 309–320.

Fileti, A.M.F., Pereira, J.A.R., 1997. Adaptive and predictive control strategies for batch distillation: development and experimental testing. Comput. Chem. Eng. 21, 1227–1231.

Gorak, A., Schoenmakers, H., 2014. Distillation: Operation and Applications. Elsevier, ISBN: 978-0-12-386876-3.

Gupta, A., Bhartiya, S., Nataraj, P., 2011. A novel approach to multiparametric quadratic programming. Automatica 47 (9), 2112–2117.

I. Gurobi Optimization, 2012. Gurobi Optimizer Reference Manual. http://www.gurobi.com,.

Herceg, M., Kvasnica, M., Jones, C., Morari, M., 2013. Multi-parametric toolbox 3.0. In: European Control Conference, pp. 502–510.

Herceg, M., Jones, C., Morari, M., 2015. Dominant speed factors of active set methods for fast MPC. Opt. Control Appl. Methods 36 (5), 608–627.

Huyck, B., Brabanter, J.D., Moor, B.D., Impe, J.F.V., Logist, F., 2014. Online model predictive control of industrial processes using low level control hardware: a pilot-scale distillation column case study. Control Eng. Pract. 28, 34–48.

Karacan, S., Hapoglu, H., Alpbaz, M., 1998. Generalized predictive control to a packed distillation column for regulatory problems. Comput. Chem. Eng. 22, 629–632.

Kawathekar, R., Riggs, J.B., 2007. Nonlinear model predictive control of a reactive distillation column. Control Eng. Pract. 15 (2), 231–239.

Kouzoupis, D., Ferreau, H.J., Peyrl, H., Diehl, M., 2015. First-order methods in embedded nonlinear model predictive control. In: European Control Conference (ECC), pp. 2617–2622.

Kvasnica, M., Takács, B., Holaza, J., Di Cairano, S., 2015. On region-free explicit model predictive control. In: Conference on Decision and Control (CDC), pp. 3669–3674.

Löfberg, J., 2004. YALMIP: A Toolbox for Modeling and Optimization in MATLAB. In: Proc. of the CACSD Conference, Taipei, Taiwan http://users.isy.liu.se/johanl/yalmip/.

Ljung, L., 1999. System Identification, Theory for the User, 2nd ed. Prentice Hall PTR, Sweden.

Martin, P.A., Odloak, D., Kassab, F., 2013. Robust model predictive control of a pilot plant distillation column. Control Eng. Pract. 21 (3), 231–241.

Meidanshahi II, V.T.A.A., 2016. Integrated design and control of semicontinuous distillation systems utilizing mixed integer dynamic optimization. Comput. Chem. Eng. 89, 172–183.

Morari, M., Lee, J.H., 1999. Model predictive control: past, present and future. Comput. Chem. Eng. 23, 667–682.

Muske, K.R., Badgwell, T.A., 2002. Disturbance modeling for offset-free linear model predictive control. J. Process Control 12, 617–632.

Muske, K.R., Badgwell, T.A., 2002. Disturbance modeling for offset-free linear model predictive control. J. Process Control 12 (5), 617–632.

Nakaiwa, M., Huang, K., Owa, M., Akiya, T., Nakane, T., Takamatsu, T., 1998. Operating an ideal heat integrated distillation column with different control algorithms. Comput. Chem. Eng. 22, 389–393.

Pannocchia, G., Rawlings, J.B., 2003. Disturbance models for offset-free model-predictive control. AIChE J. 49 (2), 426–437.

Perry, R.H., Green, D.W., 2008. Perry's Chemical Engineers' Handbook, eighth ed. McGraw Hill professional, McGraw-Hill.

Pistikopoulos, E., Diangelakis, N., Oberdieck, R., Papathanasiou, M., Nascu, I., Sun, M., 2015. PAROC: an integrated framework and software platform for the optimisation and advanced model-based control of process systems. Chem. Eng. Sci. 136, 115–138.

Pistikopoulos, E.N., 2012. From multi-parametric programming theory to MPC-on-a-chip multi-scale systems applications. Comput. Chem. Eng. 47, 57–66.

Pu, Y., Zeilinger, M., Jones, C., 2016. Complexity certification of the fast alternating minimization algorithm for linear MPC. IEEE Trans. Autom. Control 99, 1-1.

Richter, S., Jones, C., Morari, M., 2013. Certification aspects of the fast gradient method for solving the dual of parametric convex programs. Math. Methods Oper. Res. 77 (3), 305–321.

Skogestad, S., 1997. Dynamics and Control of Distillation Columns – A Tutorial Introduction.

Skogestad, S., 2007. The do's and don'ts of distillation column control. Chem. Eng. Res. Des. 85 (1), 13–23.

Spjøtvold, J., Tøndel, P., Johansen, T.A., 2005. A method for obtaining continuous solutions to multiparametric linear programs. In: IFAC World Congress, Prague, Czech Republic.

Tøndel, P., Johansen, T.A., Bemporad, A., 2003. Evaluation of piecewise affine control via binary search tree. Automatica 39 (5), 945–950.

Ullmann, F., (Master's thesis) 2011. FiOrdOs: A matlab toolbox for C-code generation for first order methods.

Volk, U., Kniese, D.-W., Hahn, R., Haber, R., Schmitz, U., 2005. Optimized multivariable predictive control of an industrial distillation column considering hard and soft constraints. Control Eng. Pract. 13 (7), 913–927, Control Applications of Optimisation.

Wang, Y., Boyd, S., 2010. Fast model predictive control using online optimization. IEEE Trans. Control Syst. Technol. 18 (2), 267–278.